10º Congresso Brasileiro de Engenharia de Fabricação
05 a 07 de agosto de 2019, São Carlos, SP, Brasil

POWDER BEAM ANALYSIS OF LASER METAL DEPOSITION COAXIAL NOZZLE VIA IMAGE PROCESSING

Doglas Negri
Saulo Melotti
Jhonattan Gutjahr
SENAI Innovation Institute for Manufacturing Systems and Laser Processing - Arno Waldemar Dohler St, 308 - Santo Antônio
89.218-153 – Joinville/SC
doglas.negri@sc.senai.br
saulo.melotti@sc.senai.br
jhonattan.gutjahr@sc.senai.br

Gustavo Reis de Ascenção
gustv.asc@gmail.com

Abstract: *With the growth of additive manufacturing applications and its importance in the worldwide manufacturing scenario, the concern about quality has gained a significant position. The understanding of all features related to the process is a key factor to control it and therefore improve its quality. Laser Metal Deposition (LMD) is one of the available technologies to build parts, clad or repair damaged surfaces. This technique is based in a powder jet, which meets with a laser beam to form a melt pool and a deposition track. It is very important to understand the behavior of this powder beam in order to assure the quality and reproducibility of the process. The focal position is one of the most important features since it is responsible for determining the diameter size of the powder jet that reaches the processed surface. The geometry of the powder stream is a consequence of many different variables, such as gas flux, particle size distribution, nozzle geometry, and others. Because of this complex set of interactions, it is difficult to preview and model the powder beam behavior. This article presents a method to characterize the powder jet geometry using a processing image algorithm capable of determining the focus position. Three different software solutions were implemented, providing a comparison between the computational results. A picture of a consistent and visible powder jet was analyzed by the three different algorithm solutions. The comparison of the processing times was carried out and served as a first parameter to analyze the computational viability for each one of the proposals.*

Keywords*: Additive Manufacturing. Laser Metal Deposition. Powder Beam. Image Processing*

1. INTRODUCTION

Laser Metal Deposition (LMD), also called Direct Metal Deposition (DMD), Laser Engineering Net-Shaping (LENS), Laser Powder Deposition (LPD), and by other diversity of names (Melo, 2015), is one of the additive manufacturing techniques used nowadays to produce 3D metallic parts layer-by-layer direct from a CAD model. According to ISO/ASTM 52900:2015 standard, LMD can be categorized as Direct Energy Deposition (DED) process, based on material consolidation, where focused thermal energy is used to fuse materials by melting as they are being deposited (ISO/ASTM, 2015).

A few years ago, additive manufacturing (AM) was just a synonym of prototypes and experimental parts. However, a lot of recent applications of this technology have been presented in different sectors of the industry, producing final and critical parts. Aerospace, Oil and Gas, Energy, Automotive, Tool-and-Die are some industrial sectors that already benefited from this technology (Milewski, 2017). The LMD process also can be used to repair and clad parts with damaged surfaces, which is commonly called Laser Cladding (Poprawe, 2011).

The LMD process uses the focused energy of a high-quality laser beam to melt a filler material, which can be supplied as powder or wire. When using powder, the material is supplied to the melting area by means of a nozzle. The geometry of the nozzle is an important feature of the process and his model and adjustment define the geometry and some properties of powder jet (Melo, 2015).

To assure the quality, repeatability and process control, it is important to know and understand the behavior of powder stream since this has a direct influence in the process results. The focus diameter of powder beam is the most important feature. However to reach the focal position is very important to know where it is located, i.e. the position in the Z-axis with the minimum diameter along the powder jet and, consequently, the region with more mass concentration.

Thus, some research efforts have been expending to create methods and develop tools to analyze the powder beam behavior, both online and offline of the process. The objective of this work is to test different approaches for automatic identification of the focal length and diameter (spot size) of a powder beam via image analysis. This work does not aim

at a full statistic validation of the proposed models, but rather at a comparison between different methodologies and their computational feasibility through the analysis of a single image sample.

2. LITERATURE REVIEW

The LMD Process is characterized by the use of a focused laser beam and powder jet, adding material to a surface and allowing it to be metallurgically bonded into the existing substrate and fused into the part being built. By manipulating the spatial locations of the melt-pool, a complete 3D article can be built spot-by-spot, line-by-line, and then layer-by-layer (Yang et al., 2017).

The spatial distribution of mass concentration along the powder beam, as well as the focal distance of powder/laser and the standoff distance (distance between the nozzle and the deposition area), are still insufficiently studied factors of the additive technologies that work by the principle of material deposition. The correct combination of these parameters is the key to a regular and controlled deposition of the LMD process (Donadello et al., 2018). Therefore, there is still a gap of knowledge to be filled regarding the dynamic interactions between powder flow and the molten pool.

Studies on the influence of process parameters (e.g. laser power and feed rate) on the molten pool and clad dimensions have been conducted by means of computational tools and real-time monitoring systems. Ocylok et al. (2014) used a CMOS camera for process monitoring and related the pool size modifications with respect to laser power and feed rate. Donadello et al. (2018) have developed a setup method based on coaxial triangulation to optimize deposition parameters in the process. Montero et al. (2016) have developed a method for real-time inspection of the mass flow rate and particle density distribution using a high-speed camera (CMOS) and a laser lighting device (laser illumination diode). In order to determine the density of particles, the authors used image processing techniques. The image taken was segmented, the background was subtracted and a threshold was applied for binarization. Based on a mathematical model, Tan et al. (2018) verified that the distance from the nozzle to the substrate determines the powder flow mass concentration on the surface of the substrate and this influences the dimensions of the deposited layer, especially the thickness. Arizzubieta et al. (2017) verified through numerical simulation that the concentration of the powder particles follows a Gaussian distribution in the focal plane, being maximum in the center of the axis. Tabernero et al. (2010) developed a mathematical model capable of calculating the powder distribution shape, particle velocities, and trajectories. The authors applied an alternative and simple method based on powder weight measurement captured at different distances from the nozzle axis to validate their model.

3. METHODOLOGY

An LMD machine (manufacturer: RPM Innovations®, model: 535) was used as the main platform for the experiments. By means of a rotating-disk powder feeder (12 rpm), 1015-00 Ni-Cu Alloy (manufacturer: Höganäs, granulometry: 20-106 µm, gas atomized, condition of use: virgin) was carried by an argon flow (6 l/min) towards a coaxial continuous nozzle and focused in a reduced working area, which presents a high powder mass concentration (consolidation plane) and is therefore normally used in LMD processes. The material mass flow carried by the powder beam in these conditions was 21 g/min. This average measurement was obtained by collecting all particles in a bag for 120 s and sequentially weighting in a precision balance. Additionally to the carrier gas, a central argon flow (40 l/min) was employed to prevent any debris from reaching the system's optics. The center purge flow has also an influence on powder beam behavior. In order to obtain high-quality images for the powder beam analysis, a photographic apparatus was mounted (camera/lens: Canon Rebel EOS T3i/135 mm, tripod, local lateral illumination, and matt dark background fabric). Figure 1 illustrates the experimental setup. After the powder flow was established, 60 s waited so that a stationary condition could be reached and a single photo was shot (aperture: f/5.6, shutter speed: 2 s, ISO speed: 100).

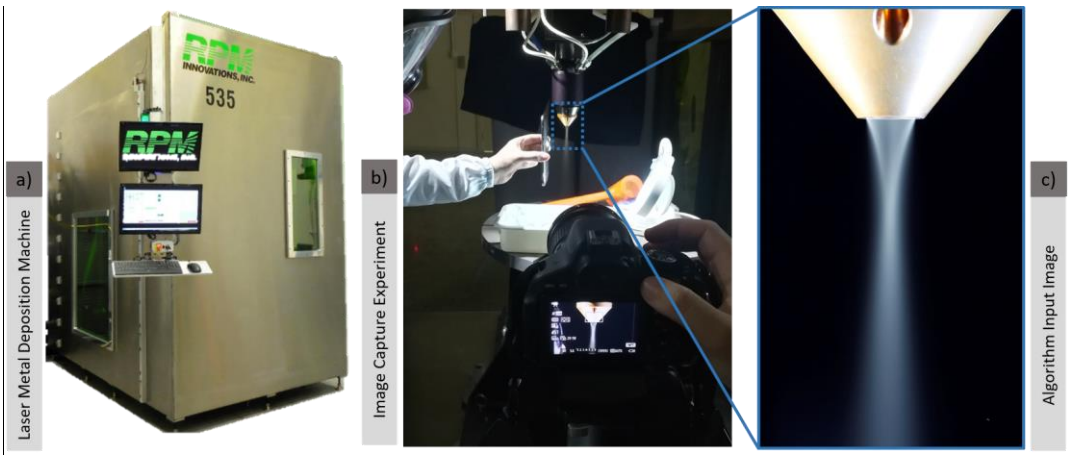

Figure 1. Image capture experiment setup.

The image obtained with the aforementioned procedure (2592x1728) served as input for three different analysis presented in this paper: one Threshold and two Gaussian methods. As already stated in the Introduction Section, the objective of this work is to test different approaches for automatic identification of the focal length and diameter (spot size) of a converging-diverging powder beam via image analysis. The first and last steps are common to all methods. Initially, the original image is imported in grayscale as a matrix (0-255) into the software Scilab 6.0.1 (incl. Image Processing and Computer Vision Toolbox) for a cropping operation. The peripheral image aspects are then removed, for the creation of a new clean, simplified image of the powder focal area. This procedure was automated with the help of the Sobel filter and mathematical operations in the region where the copper nozzle is visible at the image. The left and right edges formed by the 2D-projection of nozzle cone where identified. Simple analytic geometry calculations were implemented to find the intersection point of the baselines of each detected edge. As this point represents a first estimation of the beam focus location, the cropping box took it as a central reference. After this process, a 401x501 matrix was obtained for use in the following steps of each method. Moreover, the Sobel filtered original image also provided useful information for the calculation of mm-pixel conversion factor. The number of pixels in the nozzle top edge corresponds to the nozzle diameter, which was measured with a caliper. In this experimental setup, the conversion factor is 0,0456 mm/pixel. It will be used in the last step of each method to convert the pixel numbers representing the beam´s characteristic parameters into real lengths. Figure 2a presents the detailed steps of all methods.

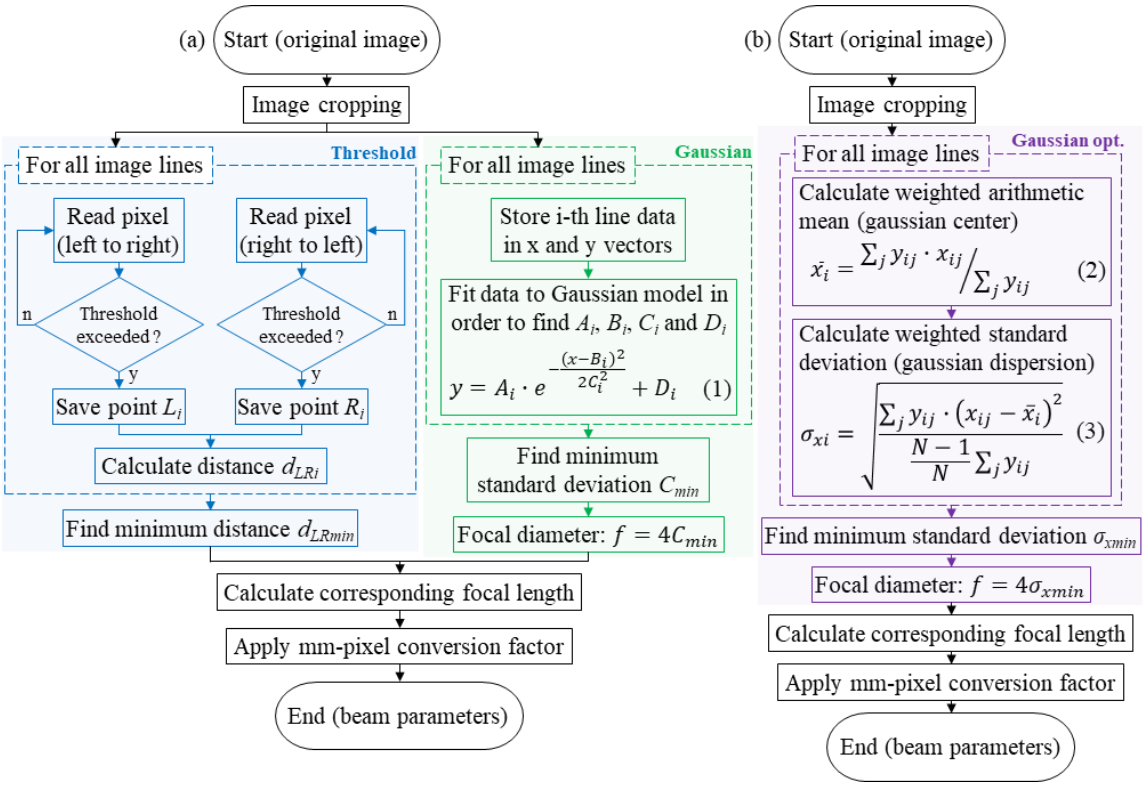

Figure 2. Algorithms' Flowchart.

The Threshold method extracts the powder beam´s characteristic parameters by drawing two isocurves that define the boundaries of an equivalent ideally shaped beam. One can basically see the powder beam because of the light reflection on the metallic particles´ surfaces. Since the particle concentration tends to be higher towards the central axis of a converging-diverging beam, the light reflection will generate brighter pixels in this region. Moreover, one can see that the pixel values change smoothly and almost monotonically at each side of the powder beam, increasing from the left towards the center and decreasing from the center to the right extremity. This regularity surrounding the focal region can be partially explained by the fact that the camera does not shoot photos instantaneously, capturing not only one position of a particle but it´s path during the acquisition time. In this sense, this method is based on the fact that the pixel values curve will always cross a defined threshold level twice: once in its growing portion and again when it decreases to a ground level. Therefore, in this method, every line of the cropped image is read in two directions (left to right and right to left) until a flag is raised when a pixel level exceeds the threshold. The distance between both flagged points (L_i and R_i) in a line corresponds to the beam diameter at that section. A search for the minimum distance of all sections (d_{LRmin}) gives the beam focal diameter. After the focus is found, its distance to the nozzle top (visible in the Sobel filtered original image) defines the focal length. Finally, both focal diameter and focal length are converted to millimeters by using the conversion factor mentioned above.

Besides the monotonically growing and decreasing behavior of the pixel values in each line of the cropped image, the Threshold method showed that the curve representing each line had a characteristic symmetric bell shape (normal probabilistic distribution). This was the motivation for the proposal of further analysis methods. The Gaussian method consists of fitting the pixel values in each column of a line into the Gaussian model (see Eq. (1) in Fig. 2a). An optimization procedure (Scilab´s function "data fit") finds the values of the constants A_i, B_i, C_i and D_i that minimize the error for the data set provided by each line of the image. These four degrees of freedoms were chosen to accommodate the following Gaussian curve´s form parameters: maximum pixel value (A_i), mean location of the curve´s maximum (B_i), curve´s dispersion or standard deviation (C_i) and vertical shift due to e.g. different background pixel levels (D_i). Once all parameters were found for every image line, a search for the minimum standard deviation (C_{min}) indicates the location of the powder beam waist (focal region). The hypotheses that the focal region presents the highest powder concentration and therefore the lowest particle dispersion was adopted to formulate this model. Commonly used to describe the propagation of Gaussian laser beams, the $1/e^2$ criterion (Herziger and Poprawe, 1998) was analogously employed in this study to describe the propagation of Gaussian powder beams. The powder beam radius is defined as the point in which the pixel value (reflection intensity) drops to $1/e^2 \approx 13{,}5\%$ of its maximum value in a certain image line. In other words, the beam radius of a certain section corresponds to twice the value of the calculated standard deviation. Therefore, the focal diameter is equal to four times the minimum standard deviation found in a cropped image. Finally, just as in the Threshold method, the focal length is calculated and both values are converted to millimeters.

As shown in the Results and Discussions Section, although the Gaussian method delivered interesting results for the characterization of the powder beam, the computer processing time was considerably high. The algorithm executes an iterative optimization process for every line of the cropped image, what could compromise the applicability of this method for images with larger dimensions and/or higher resolution. To overcome this challenge, a third method called Gaussian optimized was tested. This approach is also based on the fact that the pixel values curves have the shape of Gaussian distribution profiles, with the main difference that it does not require an iterative procedure for the calculation of the standard deviation of each image line. The statistical quantities weighted arithmetic mean and weighted standard deviation (see Eq. (2) and (3) in Fig. 2b) are determined through concise mathematical calculations (MicroStrategy, 2019). Separately for each image line (index j, total of N elements), every pixels position x_{ij} (i.e. column) is weighted by its corresponding pixel value y_{ij} (brightness), returning where the average central value is located and in how far the surrounding pixels tend to deviate from this center in terms of reflection intensity. Thus, with considerably fewer operations, the minimum standard deviation (σ_{xmin}) can be found, serving as the basis for the calculation of focal diameter and eventually focal length in this optimized method.

4. RESULTS AND DISCUSSION

All the algorithms were evaluated in the same hardware, trying to keep the same conditions. The simulations are performed using an Intel i5-2450M processor at the speed of 2.5 GHz with 16GB of RAM Memory. The results of the threshold-based detection algorithm, where three arbitrary values of this limit were studied (30, 55 and 85), can be seen in Figure 3. It is possible to observe that the change in the limit value has little influence on the focal length (18.75 mm). However, its influence is clearly perceived in the diameter of the powder focus, presenting behavior that is inversely proportional to the increase of the threshold value. It is worth noting that the average processing time of this algorithm is about 6.33 seconds. Since the algorithm output strongly depends on the selected threshold value, this method would be sensitive to changes in powder beam parameters (e.g. powder type and particle size) and lighting conditions, therefore demanding a considerably high calibration effort in real processes application.

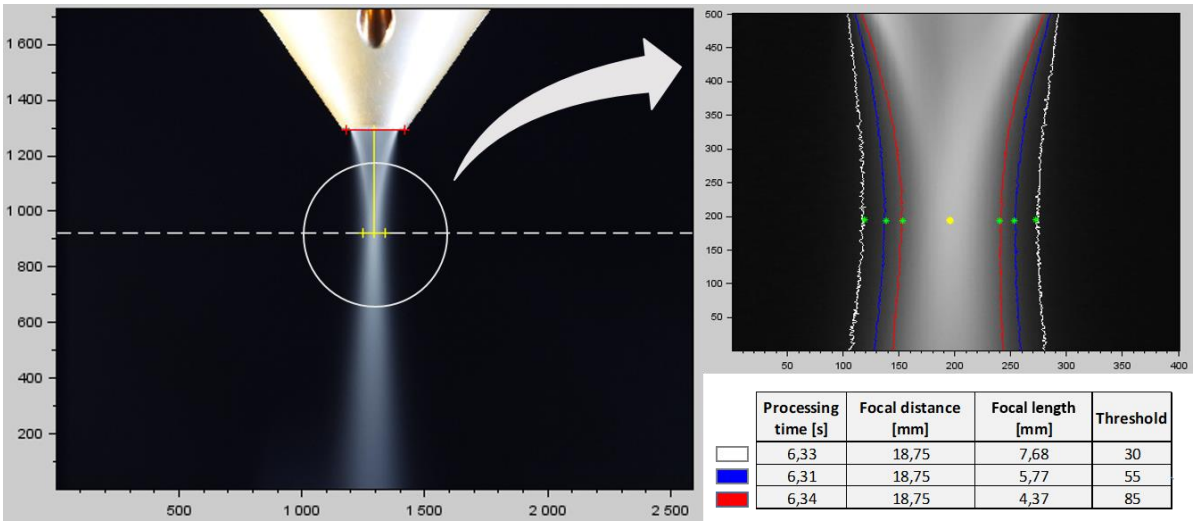

Processing time [s]	Focal distance [mm]	Focal length [mm]	Threshold
6,33	18,75	7,68	30
6,31	18,75	5,77	55
6,34	18,75	4,37	85

Figure 3. First algorithm's results.

Using the same input image, the results related to the detection algorithm based on Gaussian curve adjustment (fitting) are presented in Figure 4. In this approach, the diameter of the powder focus was calculated by the expression $4*C_{min}$. The values of 6.32 mm and 16.43 mm were obtained as results for the focal diameter and focal length, respectively. Because a curve fit is performed on each line of the image, the computational cost is considerably high for this method, reaching 2262.58 seconds for the analysis of the image selected for this work.

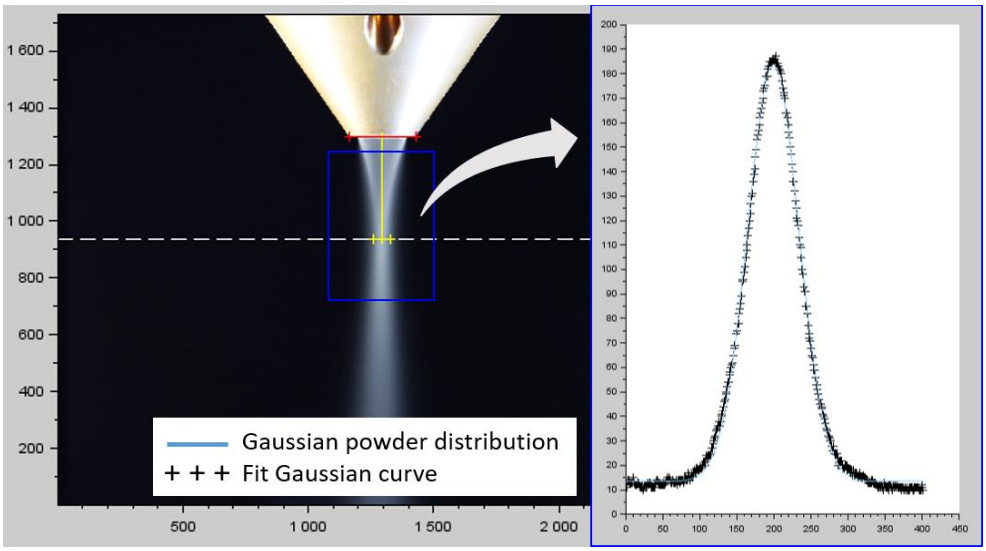

Figure 4. Second algorithm's results.

The last method is also based on the Gaussian distribution of the pixel intensities along each line of the powder beam. However, instead of using iterative fitting procedures like the Gaussian method described above, this approach finds the line corresponding to the Gaussian curve with the lowest standard deviation by means of concise mathematical operations (more information in the Methodology section). Here, the powder focus was calculated by the expression $4*\sigma_{xmin}$. Figure 5 shows the results of this technique for the same input image: a focal diameter of 6.93 mm and a focal length of 15.92 mm. This approach presents the best results from a computational point of view, with a processing time of 4.82 seconds.

In order to define the approach with the best computational efficiency, a comparison between the processing times of the three algorithms was performed. Approaches 1 and 3 presented a very similar computational cost, approximately 6.3 seconds for the 1st approach and 4.8 seconds for the 3rd algorithm. The second method is extremely costly from the computational point of view, taking approximately 2263 seconds for image processing. At this stage, it is not possible to discard any of the approaches proposed above, since the accuracy of the detected powder beam geometrical features (focal diameter and length) has not yet been evaluated. In further works, the stability of each of the proposed algorithm should be tested in a greater set of input images (different powder beam parameters and lighting conditions). Additionally, LMD experiments should be performed in order to analyze which method delivers the most suited beam parameters to perform a high quality clad deposition.

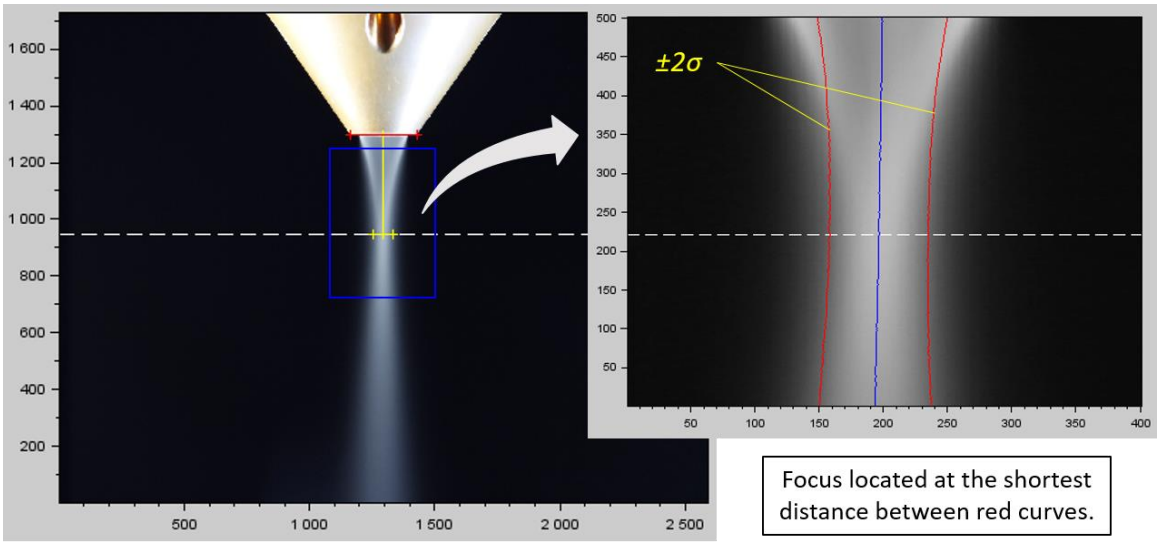

Figure 5. Third algorithm's results.

5. ACKNOWLEDGMENTS

We are grateful to the SENAI Innovation Institute for Manufacturing Systems and Laser Processing for the infrastructure offered to realize this study.

6. REFERENCES

ARRIZUBIETA, Jon Iñaki et al. *Evaluation of the relevance of melt pool dynamics in Laser Material Deposition process modeling*. International Journal of Heat and Mass Transfer, v. 115, p. 80-91, 2017.

DONADELLO, Simone et al. *Coaxial laser triangulation for height monitoring in laser metal deposition*. Procedia CIRP, v. 74, p. 144-148, 2018.

ISO/ASTM. (2015). 52900:2015 - Standard Terminology for Additive Manufacturing – General Principles – Terminology. *Iso/Astm*, *52900*, 9.

HERZIGER, G. and POPRAWE, R., 1998. Lasertechnik I. Lehrstuhl für Lasertechnik der RWTH Aachen und Fraunhofer-Institut für Lasertechnik, 2nd edition.

MELO, L. (2015). *Powder Jet Particle Density Distribuition Analysis and Qualification for the LASER Metal Deposition*. Master Thesis - Universidade Federal de Santa Catarina, Florianópolis.

MICROSTRATEGY, 2019. "Functions Reference - WeightedStDev (weighted standard deviation of a sample)" https://www2.microstrategy.com/producthelp/10.8/FunctionsRef/Content/FuncRef/WeightedStDev__weighted_standard_deviation_of_a_sa.htm - Visited on 13 Jan. 2019.

MILEWSKI, J. O. (2017). *Additive Manufacturing of Metals - From Fundamental Technology to Rocket Nozzles, Medical Implants, and Custom Jewelry*. Springer International Publishing, Santa Fe, 1st Edition.

MONTERO, Javier et al. *Inspection of Powder Flow During LMD Deposition by High-Speed Imaging*. Physics Procedia, v. 83, p. 1319-1328, 2016.

OCYLOK, Sörn et al. *Correlations of melt pool geometry and process parameters during laser metal deposition by coaxial process monitoring*. Physics Procedia, v. 56, p. 228-238, 2014.

POPRAWE, R. (2011). *Tailored Light 2*. Springer-Verlag, Aachen, 1st Edition.

TABERNERO, I. et al. *Numerical simulation and experimental validation of powder flux distribution in coaxial laser cladding*. Journal of Materials Processing Technology, v. 210, n. 15, p. 2125-2134, 2010.

TAN, Hua et al. *Process mechanisms based on powder flow spatial distribution in direct metal deposition*. Journal of Materials Processing Technology, v. 254, p. 361-372, 2018.

YANG, L., Hsu, K., Baughman, B., Godfrey, D., Medina, F., Menon, M., & Wiener, S. (2017). *Additive Manufacturing of Metals: The Technology, Materials, Design and Production*. Springer international publishing, Birmingham, 1st Edition.

7. RESPONSIBILITY NOTICE

The authors are the only responsible for the printed material included in this paper.